

RESEARCH PAPER

Evaluation of the Effectiveness of Palladium (II) Complex with a New Ligand Derived from 2-Hydrazinylbenzoxazole and 2-Aminothiazole in Anticancer Activity

Falah Haasan Hadi, Hayder Obaid Jamel *

Department of Chemistry, College of Education, University of AL-Qadisiyah, Iraq

ARTICLE INFO

Article History:

Received 05 April 2025

Accepted 05 June 2025

Published 01 July 2025

Keywords:

Anticancer

Benzoxazole

Complex

Thiazole

ABSTRACT

The new 2-(2-(benzoxazole-2-yl)-hydrazinildene)-2,1-diphenyl-N-(thiazole-2-yl)ethane-1-amine (BOHPTEI) ligand was prepared from the mixture of 2-mercaptobenzoxazole with hydrazine dissolved in absolute ethanol to form compound-A, while the ligand was obtained in its final form from the reaction of compound-A with each of benzil and 2-aminothiazole. The Pd (II) complex was prepared through the reaction between palladium chloride and BOHPTEI ligand. The structures of the prepared ligand and its complex has been characterized using a variety of spectroscopic techniques such as FT-IR, UV-Visible, and ¹H-NMR, FE-SEM, atomic absorption, molar conductivity, elemental microanalysis, magnetic susceptibility measurements, and melting points. The azomethine of the benzoxazole and thiazole rings, as well as the nitrogen atoms of the azomethine groups of the schiff base, were found to coordinate with the metal ion in the FTIR spectrum of the ligand. Depending on the UV-Visible and magnetic sensitivity measurements, the complex had a square planar geometry. Further measurements have proven that the Pd (II) complex can be used in an anti-cancer activity.

How to cite this article

Hadi F, Jamel H. Evaluation of the Effectiveness of Palladium (II) Complex with a New Ligand Derived from 2-Hydrazinylbenzoxazole and 2-Aminothiazole in Anticancer Activity. J Nanostruct, 2025; 15(3):896-907. DOI: 10.22052/JNS.2025.03.008

INTRODUCTION

Benzoxazole is an important class of heterocyclic compounds [1]. Due to different biological and pharmacological properties, benzoxazole and its derivatives are used as anti-inflammatory, antibacterial [2], antiviral, anti-tuberculosis [3], antispasmodic and antidepressant [4], cardiovascular stimulant [5], pharmaceutical applications, and medicinal chemical discovery programs [6]. These compounds are also used in the synthesis of bioactive substances such as lactams [7]. Benzoxazoles is also used to combat

oxidative stress and to prevent many diseases such as types of cancer in many clinical processes [8-10]. Benzoxazole, known as 1,3-benzoxazole, is an aromatic organic heterocyclic compound consisting of an oxazole ring, one oxygen atom and one nitrogen atom attached to the benzene ring [11, 12]. It was first reported by chemist Haritzsch in 1887 AD. Molecular formula of C₇H₅NO, molar mass of 119.12 g/mol, melting point of 27-30°C, and boiling point of 182° [13-15] were reported for this compound. It has a white to light yellow color with a pyridine-like odor, insoluble in

* Corresponding Author Email: haider.hassani@qu.edu.iq



water, at the same time it dissolves completely in organic solvents like ethanol [16, 17]. In general, benzoxazole and its derivatives are employed in coordination chemistry for the production of complexes [18, 19], and other applications such as photoluminescence and bleaching and dyeing [20, 21]. Thiazole is a five-membered heterocyclic compound containing nitrogen and sulfur at positions 1 and 3, respectively. Thiazoles have diverse biological activities, such as anti-inflammatory [22, 23], anti-fungal, anti-cancer, anti-bacterial, anti-spasmodic, anti-viral, and anti-tumor [22, 24]. This diversified activity generated the investigations with preparation of new derivatives of thiazoles [25]. A thiazole is a pale yellow liquid with a pyridine-like odor, which its molecular formula is C_3H_3NS with a boiling point of 116 -118 °C, soluble in alcohol [22]. Thiazoles are part of many natural compounds, like vitamin B1 [26].

This study involved the preparation of the new ligand 2-(2-(benzoxazole-2-yl)-hydrazinyldine(-2,1-diphenyl-N-(thiazole-2-yl)ethane-1-amine (BOHPTEI)] Schiff base type and its complex with the Pd (II) to study the biological activity of the prepared ligand and its complex in anti-cancer fields.

MATERIALS AND METHODS

Chemicals and methods

Chemical reagents were supplied by Sigma-Aldrich, Merck, MSDS, and BDH companies. UV-visible spectra were obtained in the wavelength from 200 to 1000 nm using a Shimadzu UV-165PCS spectrophotometer. NMR results were recorded on a Varian transform Fourier spectrometer, running at 300 MHz with tetramethyl silane as the internal reference standard in DMSO-d₆ solvent. FTIR spectra were recorded in the range of 400-4000 cm^{-1} employing an FTIR 8400S Shimadzu spectrophotometer (Japan). The melting points of prepared samples were obtained employing the Stewart melting point. The magnetic susceptibilities at room temperature were measured with a Balance Magnetic Susceptibility Model MSB-MKI. The atomic absorption spectrophotometry was performed employing a Shimadzu AA-6300 instrument to determine the metal content. The FESEM images of the prepared compounds were recorded using the (MIRA3 TESCAN, Czech), while the XRD measurements were employed using the (D2Phaser Bruker AXS GmbH) with an angular

range of $2\theta=20-80^\circ$. Conductivity were measured at a concentration of ($1 \times 10^{-3}M$) and at laboratory temperature, using the Digital Conductivity Series Ino device. Cond 3110 SET1 using ethanol as a solvent. Lastly, elemental analysis was performed using the EA-300.mth instrument.

Synthesis of the ligand (BOHPTEI)

The BOHPTEI ligand was synthesized in the following two stages:

Preparation of the 2-hydrazinylbenzoxazole (A) is the initial step. The 2-hydrazinylbenzoxazole (A) compound was made through the reaction between 1.5 g (0.01 mol) of the 2-mercaptobenzoxazole in 25 mL of absolute ethanol as a solvent in a round flask (250 mL), and then adding 5 mL (0.01 mol) aqueous hydrazine with 15 mL of absolute ethanol under stirring continuously. The solution was treated under a reflux process for 8 h. The precipitate was then collected and dried to produce yellow crystals, and the product was then recrystallized from chloroform to remove any unreacted substances. The precipitate was dried in the next step, as it gave a yield of (35%), with a melting point of (102 °C).

The second step is synthesis of the BOHPTEI ligand. 1.5 g (0.01 mol) of compound A was dissolved in 25 mL of absolute ethanol as a solvent under continuous stirring at a temperature of 40-50 °C. Next, a solution of 2.1 g (0.01 mol) of benzil dissolved in 25 mL of absolute ethanol, was acidified by adding 5-6 drops of glacial acetic acid. After that, a solution 1.0 g (0.01 mol) of 2-aminothiazole was added. The mixture was continually refluxed for 8 h. The solution was cooled, and a precipitate was seen. It was obtained by recrystallizing 99.9% ethanol, collecting the precipitate (yield: 73%), and measuring it at 95-98 °C. Fig. 1 showed the preparation of the BOHPTEI ligand.

Synthesis of the palladium (II) complex

0.423g (0.001 mol) of the BOHPTEI ligand was dissolved in 10 mL of absolute ethanol, followed by the addition of 0.177g (0.001mol) of palladium (II) chloride. After 2 h of refluxing under stirring, precipitates were produced, filtered, dried, and then recrystallized. Table 1 included some the physical properties of the prepared ligand (BOHPTEI) as well as palladium (II) complex.

Cytotoxic studies-MTT assay

By using an in vitro MTT cytotoxicity assay on

breast cancer cell lines (MCF-7) grown in Dulbecco's modified Eagle's medium (DMEM) supplemented with 10% fetal bovine serum (FBS; Gibco) and 1% penicillin-streptomycin, the cytotoxicity of the BOHPTEI ligand and Pd (II)-complex was investigated. The MTT test was modified to determine cell viability by incubating at 37 °C in a humidified environment with 5% (v/v) CO [27]. For 24 h, cells were seeded at a density of 104 cells/well in 96 dishes). The medium was extracted after 24 h incubation at 37 °C, and cells were treated with different concentrations (0, 50, 100, 200, 400, 800 and 1600 µg/ mL) after a 72-h incubation

period at 37 °C. The medium was then withdrawn from the board. Each became full of 100 µL of MTT reagent (1 mg/ mL) in serum-free medium. After 4 h of incubation, the medium was removed, and 200 µL of dimethyl sulfoxide (DMSO) were applied to each well. The absorbance of the MTT metabolite dissolved in DMSO was determined employing a microplate reader at a wavelength of 570 nm. There had three inspections for every concentration. % Inhibitory concentrations of 50% (IC50) were determined, cellular viability was estimated, and IC50 curves were generated using the x-dose response equation [28].

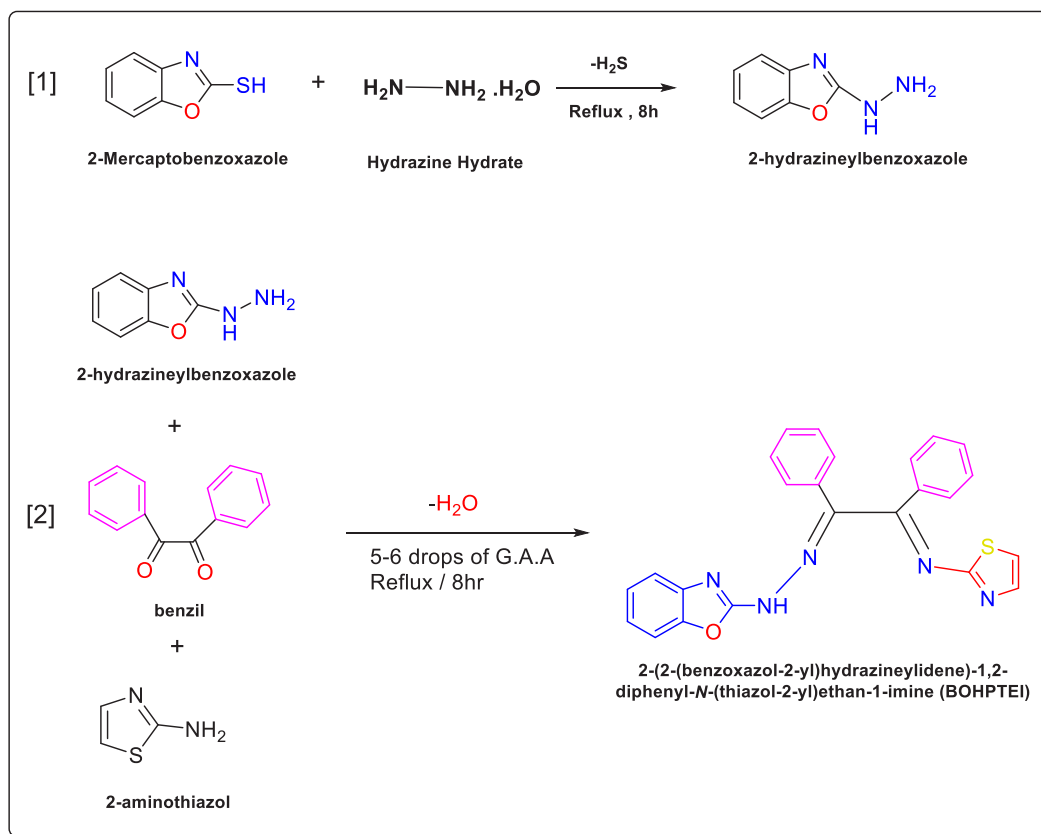


Fig. 1. Preparation of the BOHPTEI ligand.

Table 1. Physicochemical characteristics of BOHPTEI ligand and its palladium (II) complex.

Compounds	Color	M.p (C°)	Yield%	M.Wt
Ligand (BOHPTEI)	Light yellow	95 - 98	73	423.49
Pd- Complex	Dark brown	150 - 154	90	600.81

RESULTS AND DISCUSSION

The palladium (II) complex is dark brown, while the BOHPTEI ligand is represented as pale yellow crystals. The ligand and palladium (II) complex are soluble in several solvents, including ethanol, methanol, DMSO, and DMF, but they are insoluble in water and ether.

The ratio of ligand to metal was ascertained to be 1:2 employing the molar ratio method developed by the scientist (June) [29].

Molar conductivity Measurements

Ethanol was utilized as a solvent to measure molar conductivity at laboratory temperature and concentration (1×10^{-3} M). The molar conductivity value of palladium (II) complex is $78 \text{ ohm}^{-1} \text{ cm}^2 \text{ mol}^{-1}$). This value indicates that the complex is ionic with a ratio of 1:2 [30].

¹H-NMR spectrum of the ligand (BOHPTEI)

Fig. 2 displays the proton NMR spectrum of the

BOHPTEI ligand. Dimethyl sulfoxide (DMSO-d6) as solvent and tetramethyl silane (TMS) as a standard reference were used to measure the ¹H-NMR spectrum of at laboratory temperature [31]. The ¹H-NMR spectrum of the BOHPTEI ligand displayed a multiple signal at a chemical displacement of (M, ⁴H, $\delta = 7.37 - 7.49 \text{ ppm}$) indicating the protons of the benzoxazole ring [32]. The two protons of the thiazole ring gave a doublet signal at (D, ²H, $= 7.50 - 7.75 \text{ ppm}$) [33]. While the multiple signals at the chemical shift (M, ¹⁰H, $\delta = 7.80 - 7.97 \text{ ppm}$) belong to the protons of the two phenyl rings of benzil [34]. The singlet signal at (S, ¹H, $\delta = 8.92 \text{ ppm}$) belongs to the proton of the secondary amine group (-NH) [35]. A singlet signal at the chemical shift of 2.52 ppm resulted from the protons of the solvent (DMSO-d6) [36].

FTIR spectra of the ligand BOHPTEI and palladium (II) complex

Potassium bromide was used to compare the

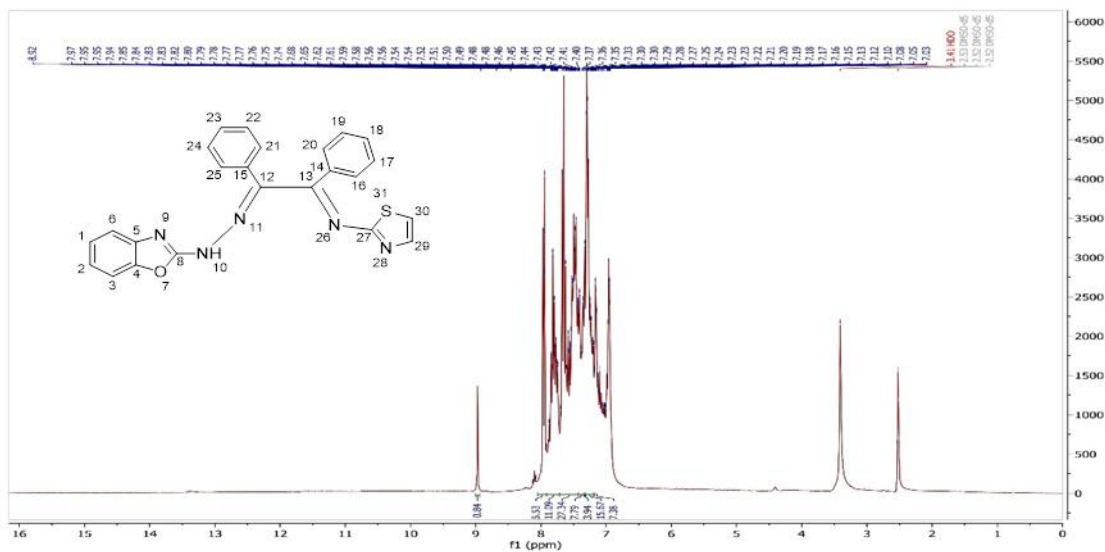


Fig. 2. ¹H-NMR spectrum of the ligand (BOHPTEI).

Table 2. Spectral bands of BOHPTEI ligand and Pd(II) complex.

Sample	ν (N-H) 20Amine	ν (C-H) Aromatic	ν (C=N) Imine	ν (C=N) Thiazole	ν (C=N) Benzoxazole	ν (C=C) aromatic	ν (M-N)
Ligand(BOHPTEI)	3301	3062	1666	1650	1604	1527 1496	-
[Pd(BOHPTEI)]Cl ₂	3294	3062	1654	1632	1594	1542 1440	516



FTIR spectra of the BOHPTEI ligand and its complex in Fig. 3 and Fig. 4. The FTIR spectrum of the free ligand displayed a clear absorption band at (3301 cm^{-1}) indicating the secondary amine group $\nu(\text{N-H})$ [37]. The band at 1666 cm^{-1} belongs to the azomethine group band ($\text{C}=\text{N}$) of the Schiff base [38, 39], while the carbonyl group disappears in the reactants. Other bands appeared at 1650 and 1604 cm^{-1} are due to the groups of azomethine of the thiazole and benzoxazole rings, respectively [40]. While, the two functional groups of $\text{C}=\text{C}$ and C-H aromatic were concentrated at 1527, 1496 cm^{-1} and 3062 cm^{-1} , respectively [41]. Additional bands appeared at 1172 and 1072 cm^{-1} are related to the functional groups of $\nu(\text{C-N})$ and (C-O) of the thiazole and benzoxazole rings, respectively [41]. In the spectrum of the prepared complex,

the azomethine group $\nu(\text{C}=\text{N})$ of the Schiff base shifted towards a lower frequency and was reported as 1654 cm^{-1} [42]. Also, the frequency of the two azomethine groups belonging to the thiazole and benzoxazole rings shifted to a lower frequency, and they occurred at 1632 and 1594 cm^{-1} in the spectrum of the prepared complex. The interaction of the ligand with the palladium ion *via* the azomethine groups of nitrogen atoms is strongly supported by these shifts [43]. A new band at 516 cm^{-1} identifies the group of M-N [44, 45]. In Table 2, the spectral bands of both samples have been listed.

Electronic spectra

As illustrated by Fig. 5, three absorption peaks could be seen in the ligand's electronic

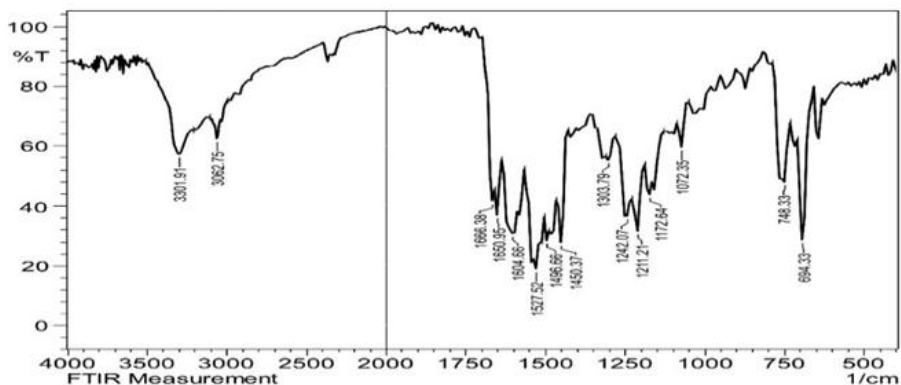


Fig. 3. FTIR spectrum of the ligand (BOHPTEI).

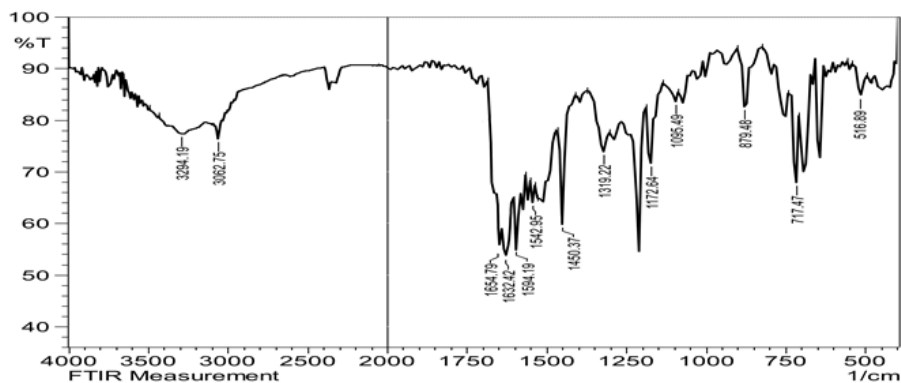


Fig. 4. FTIR spectrum of the Pd(II) complex.

spectra. Two peaks at 204 nm (49020 cm⁻¹) and 222 nm (45045 cm⁻¹) belong to the transition (π-π*), while another peak at 263 nm (38023 cm⁻¹) is due to the n-π* transition of the azomethine group (C=N) [46]. The spectrum of palladium (II) complex displayed many absorption peaks at 211 nm (47393 cm⁻¹) and 268 nm (37313 cm⁻¹). The absorption peaks at 546 nm (18315 cm⁻¹), 602 nm (16611 cm⁻¹) and 694 nm (14409 cm⁻¹) indicate the electronic transitions of ¹A_{1g}→¹E_g, ¹A_{1g}→¹B_{1g} and ¹A_{1g}→¹A_{2g}, respectively, which provide that the complex geometry is a square planar [37]. The magnetic sensitivity measurements proposed that the complex has diamagnetic properties [47]. Table 3 summarizes the electronic structure, magnetic and geometry of both samples.

XRD study

XRD measurement was employed to study the crystal structures and crystal size of the

synthesized BOHPTEI ligand and its palladium (II) complex (Fig. 6). To determine the degree of purity and the crystalline nature of samples, microstrains, and dislocation density were also calculated. There are some diffraction peaks such as micro-strains caused by crystal distortions, an absence of lattice deformation and faulting, the crystal's domain size, and the distribution of field size [48]. The XRD pattern revealed the existence of peaks, which is an indication of a crystal lattice, and broad peaks, which signify an amorphous structure. These peaks' sharpness is determined by the crystal structure, the crystal lattice properties, the crystalline levels, and other factors [49]. The crystal sizes of the synthesized BOHPTEI ligand and palladium (II) complex was determined using the Debye-Scherer formula as below:

$$D = \frac{k\lambda}{\beta \cos\theta} \tag{1}$$

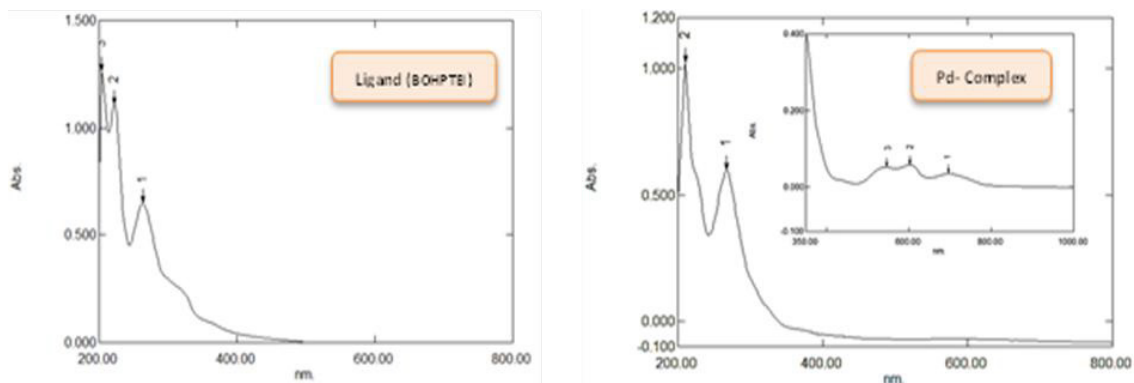


Fig. 5. UV-Vis spectra of BOHPTEI ligand and palladium (II) complex.

Table 3. Peak absorption values, magnetic momentum and expected geometry for BOHPTEI ligand and Pd(II) complex.

Compounds	λ (nm)	ν (cm ⁻¹)	Transitions	μ _{eff} (B.M)	Geometry
Ligand(BOHPTEI)	204	49020	π-π*	-	-
	222	45045	π-π*		
	263	38023	n-π*		
[Pd(BOHPTEI)]Cl ₂	211	47393	Intra Ligand	(Dia.)	Square planar dsp ²
	268	37313	Intra Ligand		
	546	18315	¹ A _{1g} → ¹ E _g		
	602	16611	¹ A _{1g} → ¹ B _{1g}		
	694	14409	¹ A _{1g} → ¹ A _{2g}		



where, D is average crystal size, k represents shape factor (0.9), λ is the wavelength of the X-ray ($\text{CuK}\alpha = 1.54056 \text{ \AA}$), β displays total width at half height FWHM, and θ is the deviation angle.

Also, the following equation was used to calculate the microcompliance:

$$S = \beta \cos \theta / 4 \tag{2}$$

where S is microstrains and β introduces total width at half-maximum height.

The density of dislocations is estimated using the formula that follows the equation.

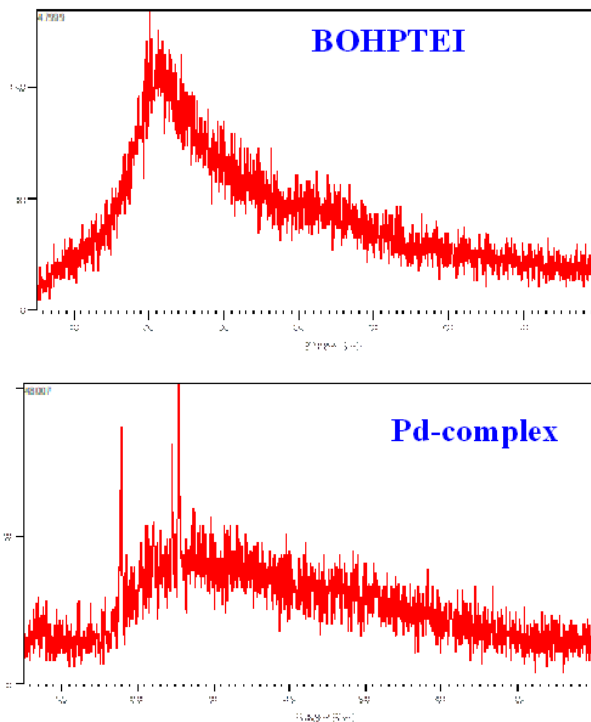


Fig. 6. XRD patterns of ligand (BOHPTEI) and its prepared metal complex.

Table 4. Interplanar distances and the 2 θ value of each peak, relative intensity for ligand and complex.

Compound	No.	Pos. °2 θ . (Radian)	Width FWHM	d-spacing A°	D Crystallite size(nm)	Intensity I_n	Rel. Int[%]
Ligand(BOHPTEI)	1-	20..3121	0.1080	4.3685	78.08	159	100%
	2-	24.2719	0.1080	3.664	78.61	156	86.46%
	3-	31.840	0.228	2.81057	37.86	155	100%
[Pd(BOHPTEI)]Cl ₂	1-	17.1860	0.236	4.9786	36.50	93	54%
	2-	24.529	0.242	3.6291	35.39	90	100%
	3-	25.394	0.1574	3.5074	54.20	98	14%

$$\delta = 1/D^2 \quad (3)$$

where δ is density of dissolutions and D shows average crystal size of samples.

The difference in distance between the crystalline degrees d of the ligand and its synthesized metallic complex, as well as the

density of dissolutions, was confirmed by Table 4. It was also found that there is an inverse relationship between the crystal size, the micro-compliantness, and the density of dissolutions [50]. XRD measurements of the BOHPTEI ligand showed a crystal size of 64.85 nm. Also, the palladium (II) complex illustrated a crystalline size of 42.03 nm.

Table 5. Evaluation of BOHPTEI on the MCF-7 cancer cell line following a 24 h incubation period at 37°C, and the HEK-293 cell line for cytotoxicity.

Concentration $\mu\text{g/ml}$	Normal cell HEK293		Cell inhibition %	Cancer cell MC7-7		Cell inhibition %
	Cell Viability			Cell Viability		
	mean	SD		mean	SD	
0	100	0	0	100	0	0
50	80/8	1/27279	19.2%	87/9	1/69705	12.1%
100	56/15	0/77781	43.85%	45	0/42426	55%
200	31/85	2/61629	70.0%	23/8	0/14142	76.2%
400	25/45	1/76776	73.3%	22/8	0/70710	77.2%
800	21/35	0/91923	78.0%	19/6	3/2526	80.4%
1600	14/45	0/35355	85.8%	10/25	3/18198	89.8%
IC50		67.5			63.1	

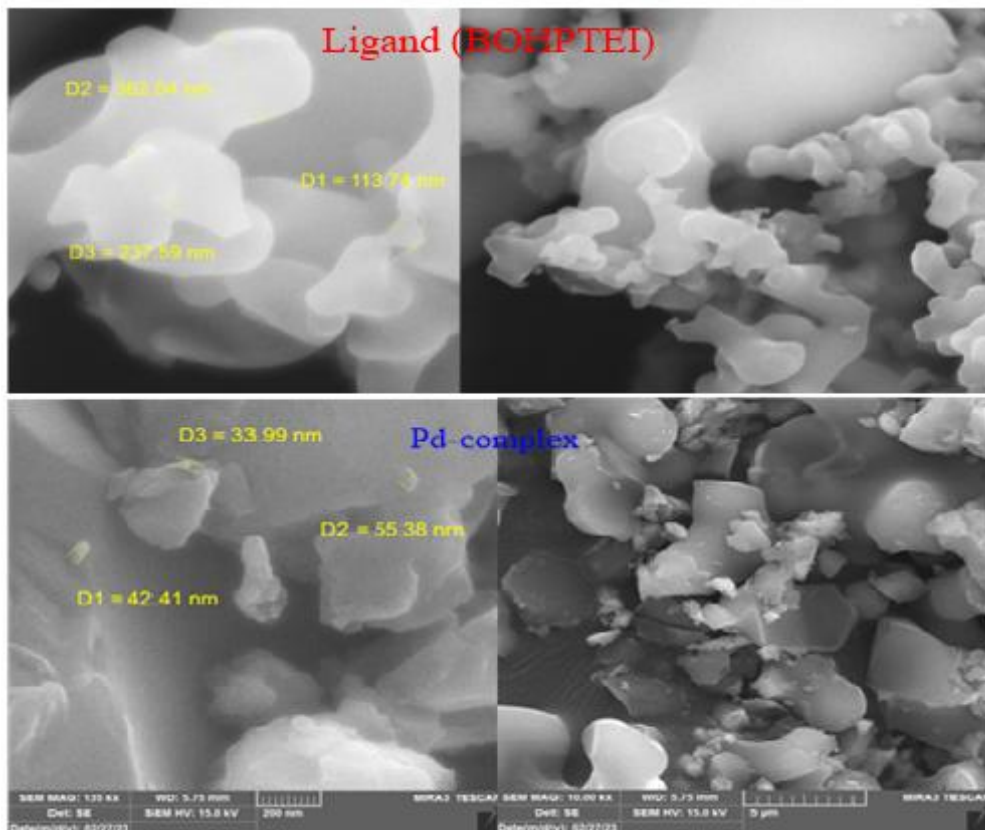


Fig. 7. FESEM images of BOHPTEI ligand and prepared metal complex.

These values indicate that the prepared BOHPTEI ligand and its palladium (II) complex have a size of less than 100 nm, meaning that they are within the nanoscale range [51].

FE-SEM study

FESEM analysis was employed to analysis the surface properties of the BOHPTEI ligand and its metal complex prepared with palladium (II) ion, in terms of particle shape, size and distribution (Fig. 7). By analyzing the FE-SEM images, the BOHPTEI ligand showed in the form of large homogeneous crystals with a particle size of 237.79 nm, while the FE-SEM image analysis of palladium (II) complex

appeared to contain irregular and inhomogeneous oval shapes with an average size of 43.93 nm. The results showed that the prepared ligand is introduced as particle size greater than 100 nm, and the prepared complex with size of less than 100 nm. These results enabled us to study the ligand and palladium (II) complex in the field of medicine and their ability to eliminate many types of cancer, including breast cancer [52].

Effect of BOHPTEI ligand and palladium (II) complex on the growth process of breast cancer cell line MCF7 and normal cells (HEK)

The effect of BOHPTEI ligand were investigated

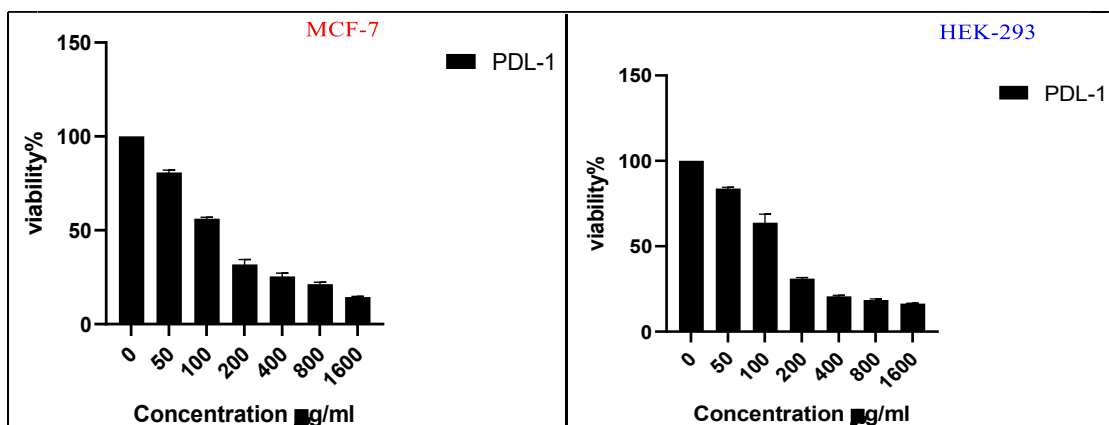


Fig. 8. % Cell viability for ligand in MCF-7 cancer cell line and the normal cells HEK-293.

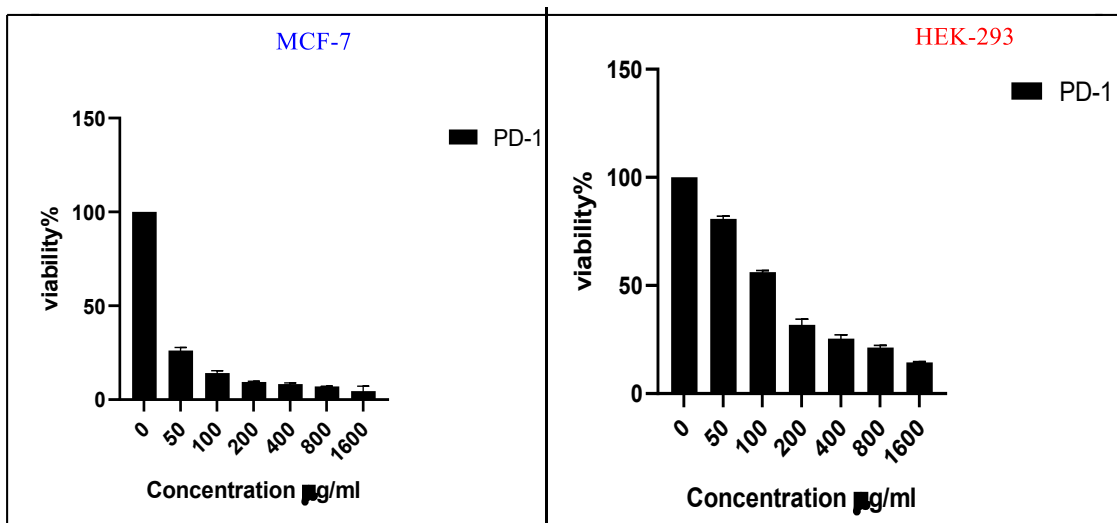


Fig. 9. % Cell viability of Pd (II) complex in MCF-7 cancer cell line and the normal cells HEK-293.

Table 6. Evaluation of the Pd (II) complex's cytotoxicity in the HEK-293 and MCF-7 cancer cell lines after a day of incubation at 37°C.

Concentration µg/ml	Normal cell HEK-293		Cell inhibition %	Cancer line cells MCF-7		
	Cell Viability			Cell Viability		Cell inhibition %
	mean	SD	Mean	SD		
0	100	0	0	100	0	0
50	80/8	1/57523	19.2	26/2	1/55563	73.8
100	56/15	1/38524	43.85	14/15	1/34350	85.85
200	31/85	8/21442	68.15	9/4	0/42426	90.6
400	25/45	6/94603	74.55	8/25	0/63639	91.75
800	21/35	4/30556	78.65	7	0/14142	93
1600	14/45	2/44673	85.55	4/5	2/68700	95.5
IC50	150 µg			0.278		

on the the development of breast cancer cell MCF7 and healthy cell HEK (Table 5 and Fig. 8). The highest rate of inhibition occurred at a concentration of 1600 µg/mL, while the lowest rate of inhibition of the growth of breast cancer cells was detected at a dosage of 50 µg/mL. In contrast, the lowest and highest rates of inhibition of normal cell development (HEK) were 50 and 1600 µg/mL, respectively. To assess the potential for employing these chemicals as a potential treatment, normal cells (HEK) were employed to compare with breast cancer cells. The greatest inhibition rate for breast cancer cells was discovered to be 89.8% at a dosage of 1600 µg/mL. The normal cell line's inhibition rate in the same concentration was 85.8%, which is a reasonably decent result, but certain changes are required to raise this rate. According to these results, the half-maximal inhibitory concentration (IC50) of breast cancer cell line was 63.1 µg/mL, while for normal cells (HEK) the IC50 was equal to 67.5 µg/mL. This also reinforces the good results obtained using the BOHPTEI ligand in the treatment of breast cancer [53]. On the other hand, palladium (II) complex inhibited the growth of cancer cells MCF7 by (95.5%) at a concentration of 1600 µg/mL, while it was less inhibiting on normal cells (HEK-293) at this concentration, as it gave an inhibition rate of 85.55% (Table 6 and Fig. 9). The values of IC50 for cancer cell line were IC50= 0.278 µg/mL, while it gave an equal value to IC50= 150 µg/mL with normal cell lines [54, 55].

CONCLUSION

In this research, the BOHPTEI ligand was prepared from 2-mercaptobenzooxazole and

2-aminothiazole. Also, Pd (II) complex was fabricated by reaction this ligand with divalent palladium chloride. These compounds were characterized by in a variety of spectroscopic and physical methods. The FTIR spectra confirmed the formation of the azomethine group. These spectra also demonstrated that the ligand coordinates with the palladium ion through the nitrogen atoms of the two azomethine groups of the Schiff base as well as the two azomethine groups of the benzoxazole and thiazole rings. When coordinated, the azomethine group shifted towards lower frequencies as compared to the free ligand. The electronic results of Pd (II) complex suggested that the complex has a square planar geometry. Molar conductivity measurements showed that Pd (II) has an ionic nature. XRD and FESEM analyses proved that the ligand and its complex have a nanoscale size. Also, MTT assay of both ligand and Pd (II) complex against breast cancer cell line (MCF-7) and normal cells (HEK) illustrated promising anticancer activity.

CONFLICT OF INTEREST

The authors declare that there is no conflict of interests regarding the publication of this manuscript.

REFERENCES

1. Kumar KR, Satyanarayana PVV, Srinivasa Reddy B. NaHSO₄-SiO₂-Promoted Solvent-Free Synthesis of Benzoxazoles, Benzimidazoles, and Benzothiazole Derivatives. *Journal of Chemistry*. 2012;2013(1).
2. Ghoshal T, Patel TM. Anticancer activity of benzoxazole derivative (2015 onwards): a review. *Future Journal of Pharmaceutical Sciences*. 2020;6(1).
3. Kokkiligadda SB, Musunuri S, Maiti B, Rao MVB, Somaiah N. Synthesis and biological evaluation of amide derivatives of

- quinazoline-thiazole-oxazole as anticancer agents. *Chemical Data Collections*. 2023;48:101046.
4. H. Sultan A. Synthesis and Identification of some Benzoxazole Derivatives via Mannich Reaction. *Rafidain Journal of Science*. 2014;25(6):49-54.
 5. Chang W, Sun Y, Huang Y. One-pot green synthesis of benzoxazole derivatives through molecular sieve-catalyzed oxidative cyclization reaction. *Heteroat Chem*. 2017;28(2).
 6. Mnguni MJ, Lemmerer A. A structural study of 4-aminoantipyrine and six of its Schiff base derivatives. *Acta Crystallographica Section C Structural Chemistry*. 2015;71(2):103-109.
 7. Mahmood Yousif Al-Labban H, Mohammed Sadiq H, Abduljabbar Jaloob Aljanaby A. Synthesis, Characterization and study biological activity of some Schiff bases derivatives from 4-amino antipyrine as a starting material. *Journal of Physics: Conference Series*. 2019;1294(5):052007.
 8. Kumar S, Rathore DS, Garg G, Khatri K, Saxena R, Sahu SK. Synthesis And Evaluation of Some Benzothiazole Derivatives as Antidiabetic Agents. *International Journal of Pharmacy and Pharmaceutical Sciences*. 2017;9(2):60.
 9. Sajeesh S, Sharma CP. Mucoadhesive hydrogel microparticles based on poly (methacrylic acid-vinyl pyrrolidone)-chitosan for oral drug delivery. *Drug Deliv*. 2010;18(4):227-235.
 10. Kianipour S, Razavi FS, Hajizadeh-Oghaz M, Abdulsahib WK, Mahdi MA, Jasim LS, et al. The synthesis of the P/N-type NdCoO₃/g-C₃N₄ nano-heterojunction as a high-performance photocatalyst for the enhanced photocatalytic degradation of pollutants under visible-light irradiation. *Arabian Journal of Chemistry*. 2022;15(6):103840.
 11. Ramineni S, Kannasani RK, Peruri VVS. Efficient one-pot synthesis of benzoxazole derivatives catalyzed by Zinc triflate. *Green Chemistry Letters and Reviews*. 2014;7(1):85-89.
 12. Kakkar S, Tahlan S, Lim SM, Ramasamy K, Mani V, Shah SAA, et al. Benzoxazole derivatives: design, synthesis and biological evaluation. *Chem Cent J*. 2018;12(1):92-92.
 13. Porcelli L, Gilardi F, Laghezza A, Piemontese L, Mitro N, Azzariti A, et al. Synthesis, Characterization and Biological Evaluation of Ureidofibrate-Like Derivatives Endowed with Peroxisome Proliferator-Activated Receptor Activity. *J Med Chem*. 2011;55(1):37-54.
 14. Chikhale RV, Pant AM, Menghani SS, Wadibhasme PG, Khedekar PB. Facile and efficient synthesis of benzoxazole derivatives using novel catalytic activity of PEG-SO 3 H. *Arabian Journal of Chemistry*. 2017;10(5):715-725.
 15. Mahmood Taher A, Ali Kadhim Kyhoiesh H, Shakir Waheeb A, Al-Adilee KJ, Jasim LS. Synthesis, characterization, biological activity, and modelling protein docking of divalent, trivalent, and tetravalent metal ion complexes of new azo dye ligand (N,N,O) derived from benzimidazole. *Results in Chemistry*. 2024;12:101911.
 16. Kumar A, Pal V, Mishra DK. Benzoxazole: Synthetic Methodology and Biological Activities. *International Journal of Pharmaceutical Sciences Review and Research*. 2025;85(2).
 17. Hiroki A, Taguchi M. Development of Environmentally Friendly Cellulose Derivative-Based Hydrogels for Contact Lenses Using a Radiation Crosslinking Technique. *Applied Sciences*. 2021;11(19):9168.
 18. Synthesis and Antioxidant Activities of Schiff Bases and Their Complexes: An Updated Review. *Biointerface Research in Applied Chemistry*. 2020;10(6):6936-6963.
 19. Hosseini M, Ghanbari M, Dawi EA, Mahdi MA, Ganduh SH, Jasim LS, et al. Investigations of nickel silicate for degradation of water-soluble organic pollutants. *Int J Hydrogen Energy*. 2024;61:307-315.
 20. Abd-Alzahra MR, Hatem ZM, Maged NQA, Kareem IK. Synthesis and characterization of novel metal complexes with new azo-schiff base ligand derived from sulfa drug and toxicological studies of its complexes as antibacterial. *International journal of health sciences*. 2022:5558-5573.
 21. Mahde BW, Sultan AM, Mahdi MA, Jasim LS. Kinetic Adsorption and Release Study of Sulfadiazine Hydrochloride Drug from Aqueous Solutions on GO/P(AA-AM-MCC) Composite. *International Journal of Drug Delivery Technology*. 2022;12(04):1583-1589.
 22. Synthesis and Characterization of New Schiff Base Ligand Derived from 4- aminoantipyrine and its complexes with some metal ions and Their Fluorescence Study. *International Journal of Pharmaceutical Research*. 2020;13(01).
 23. Mahdi MA, Oroumi G, Samimi F, Dawi EA, Abed MJ, Alzaidy AH, et al. Tailoring the innovative Lu₂CrMnO₆ double perovskite nanostructure as an efficient electrode materials for electrochemical hydrogen storage application. *Journal of Energy Storage*. 2024;88:111660.
 24. Jabir FA, Hamzah SK. SOX17 and RASSAF1A promoters methylation in circulation tumor cell and cell free DNA isolated from plasma in breast cancer Iraqi women patients. *Research Journal of Pharmacy and Technology*. 2018;11(5):2000.
 25. Synthesis, Characterization, Antibacterial and theoretical Studies of New 1,1'-(1,4-phenylene)bis(N-(4H-1,2,4-triazol-4-yl)methanimine) With some transition metal ions. *International Journal of Pharmaceutical Research*. 2020;12(sp2).
 26. Yasir AF, Jamel HO. Synthesis of a New DPTYEAP Ligand and Its Complexes with Their Assessments on Physical Properties, Antioxidant, and Biological Potential to Treat Breast Cancer. *Indonesian Journal of Chemistry*. 2023;23(3):796.
 27. Loffredo J, Tommarello D, Abulez T, Ao W, Teng P-n, Conrads K, et al. Integrated multi-omic analyses reveals clinical relevance of endometrial cancer cell line models. *Gynecol Oncol*. 2021;162:S11.
 28. Gasparini LS, Macedo ND, Pimentel EF, Fronza M, Junior VL, Borges WS, et al. In vitro Cell Viability by CellProfiler(®) Software as Equivalent to MTT Assay. *Pharmacogn Mag*. 2017;13(Suppl 2):S365-S369.
 29. Qazi SJS, Rennie AR, Cockcroft JK, Vickers M. Use of wide-angle X-ray diffraction to measure shape and size of dispersed colloidal particles. *Journal of Colloid and Interface Science*. 2009;338(1):105-110.
 30. El-bendary MM, Rüffer T, Arshad MN, Asiri AM. Synthesis and structure characterization of Pt(IV) and Cd(II) 1,10-phenanthroline complexes; fluorescence, antitumor and photocatalytic property. *J Mol Struct*. 2019;1192:230-240.
 31. Mishra VR, Ghanavatkar CW, Mali SN, Chaudhari HK, Sekar N. Schiff base clubbed benzothiazole: synthesis, potent antimicrobial and MCF-7 anticancer activity, DNA cleavage and computational study. *Journal of Biomolecular Structure and Dynamics*. 2019:1-14.
 32. Galal SA, Hegab KH, Kassab AS, Rodriguez ML, Kerwin SM, El-Khamry A-MmA, et al. New transition metal ion complexes with benzimidazole-5-carboxylic acid hydrazides with antitumor activity. *Eur J Med Chem*. 2009;44(4):1500-1508.
 33. Uyar Z, Degirmenci M, Genli N, Yilmaz A. Synthesis of well-defined bisbenzoin end-functionalized poly(ε-

- caprolactone) macrophotoinitiator by combination of ROP and click chemistry and its use in the synthesis of star copolymers by photoinduced free radical promoted cationic polymerization. Designed monomers and polymers. 2016;20(1):42-53.
34. Chen C, Chen C, Li B, Tao J, Peng J. Aqueous synthesis of 1-H-2-substituted benzimidazoles via transition-metal-free intramolecular amination of aryl iodides. *Molecules* (Basel, Switzerland). 2012;17(11):12506-12520.
 35. Karem Lk. Some Metal Ions Complexes Derived From Schiff Base Ligand with Anthranilic Acid: Preparation, Spectroscopic and Biological Studies. *Baghdad Science Journal*. 2020;17(1):0099.
 36. Issa YM, Hassib HB, Abdelaal HE. ¹H NMR, ¹³C NMR and mass spectral studies of some Schiff bases derived from 3-amino-1,2,4-triazole. *Spectrochimica Acta Part A: Molecular and Biomolecular Spectroscopy*. 2009;74(4):902-910.
 37. Şahin Ö, Özdemir ÜÖ, Seferoğlu N, Genc ZK, Kaya K, Aydinler B, et al. New platinum (II) and palladium (II) complexes of coumarin-thiazole Schiff base with a fluorescent chemosensor properties: Synthesis, spectroscopic characterization, X-ray structure determination, in vitro anticancer activity on various human carcinoma cell lines and computational studies. *J Photochem Photobiol B: Biol*. 2018;178:428-439.
 38. Heravi MM, Zadsirjan V. Prescribed drugs containing nitrogen heterocycles: an overview. *RSC advances*. 2020;10(72):44247-44311.
 39. Majeed HJ, Idrees TJ, Mahdi MA, Abed MJ, Batool M, Yousefi SR, et al. Synthesis and application of novel sodium carboxy methyl cellulose-g-poly acrylic acid carbon dots hydrogel nanocomposite (NaCMC-g-PAAc/ CDs) for adsorptive removal of malachite green dye. *Desalination and Water Treatment*. 2024;320:100822.
 40. Siregar AH, Setyawan BA, Marasabessy A. Flame retardant properties of composite fiberglass reinforced unsaturated polyester resin. *AIP Conference Proceedings: Author(s)*; 2018. p. 050007.
 41. Samota MK, Seth G. Synthesis, characterization, and antimicrobial activity of palladium(II) and platinum(II) complexes with 2-substituted benzoxazole ligands. *Heteroat Chem*. 2010;21(1):44-50.
 42. Sathiyaraj S, Ayyannan G, Jayabalakrishnan C. Synthesis, spectral, dna binding and cleavage properties of ruthenium(II) Schiff base complexes containing PPh₃/AsPh₃ as co-ligands. *J Serb Chem Soc*. 2014;79(2):151-165.
 43. Sattar R, Mukhtar R, Atif M, Hasnain M, Irfan A. Synthetic transformations and biological screening of benzoxazole derivatives: A review. *J Heterocycl Chem*. 2020;57(5):2079-2107.
 44. Seijas J, Vázquez-Tato M, Carballido-Reboredo M, Crecente-Campo J, Romar-López L. Lawesson's Reagent and Microwaves: A New Efficient Access to Benzoxazoles and Benzothiazoles from Carboxylic Acids under Solvent-Free Conditions. *Synlett*. 2007;2007(2):0313-0317.
 45. Batool M, Haider MN, Javed T. Applications of Spectroscopic Techniques for Characterization of Polymer Nanocomposite: A Review. *Journal of Inorganic and Organometallic Polymers and Materials*. 2022;32(12):4478-4503.
 46. Shaker S, Khaledi H, Ali H. Spectroscopic investigations and physico-chemical characterization of newly synthesized mixed-ligand complexes of 2-methylbenzimidazole with metal ions. *Chemical Papers*. 2011;65(3).
 47. Mansour FR, Danielson ND. Ligand exchange spectrophotometric method for the determination of mole ratio in metal complexes. *Microchem J*. 2012;103:74-78.
 48. Gaber M, El-Wakiel N, El-Baradie K, Hafez S. Chromone Schiff base complexes: synthesis, structural elucidation, molecular modeling, antitumor, antimicrobial, and DNA studies of Co(II), Ni(II), and Cu(II) complexes. *Journal of the Iranian Chemical Society*. 2018;16(1):169-182.
 49. Xu R, Zhao Y-H, Han Q-Z, Ning P-G, Cao H-B, Wen H. Computer-aided blended extractant design and screening for co-extracting phenolic, polycyclic aromatic hydrocarbons and nitrogen heterocyclic compounds pollutants from coal chemical wastewater. *Journal of Cleaner Production*. 2020;277:122334.
 50. Hassan MHA, Ismail MA, Moharram AM, Shoreit AAM. Phytochemical and Antimicrobial of Latex Serum of Calotropis Procera and its Silver Nanoparticles Against Some Reference Pathogenic Strains. *Journal of Ecology of Health & Environment*. 2017;5(3):65-75.
 51. El-Sonbati AZ, Diab MA, El-Bindary AA, Mohamed GG, Morgan SM, Abou-Dobara MI, et al. Geometrical structures, thermal stability and antimicrobial activity of Schiff base supramolecular and its metal complexes. *J Mol Liq*. 2016;215:423-442.
 52. Afanou KA, Straumfors A, Skogstad A, Skaar I, Hjeljord L, Skare Ø, et al. Profile and Morphology of Fungal Aerosols Characterized by Field Emission Scanning Electron Microscopy (FESEM). *Aerosol science and technology : the journal of the American Association for Aerosol Research*. 2015;49(6):423-435.
 53. Zeiger E, Hoffmann GR. An illusion of hormesis in the Ames test: Statistical significance is not equivalent to biological significance. *Mutation Research/Genetic Toxicology and Environmental Mutagenesis*. 2012;746(1):89-93.
 54. Kyhoiesh HAK, Al-Adilee KJ. Synthesis, spectral characterization, antimicrobial evaluation studies and cytotoxic activity of some transition metal complexes with tridentate (N,N,O) donor azo dye ligand. *Results in Chemistry*. 2021;3:100245.
 55. Radia ND, Alshamusi QKM, Sahib IJ, Jasim LS, Aljeboree AM, Alkaim AF. Oxidative coupling of phenylephrine hydrochloride using N,N-dimethyl-p-phenylenediamine: Stability and higher sensitivity. *AIP Conference Proceedings: AIP Publishing*; 2022. p. 030026.